J Mol Model (2003) 9:153–158
DOI 10.1007/s00894-003-0121-5

ORIGINAL PAPER

Jean-San Chia · Yu-Shuan Shiau · Po-Tsarng Huang · Yuh-Yuan Shiau · Yau-Wei Tsai · Hsiou-Chuan Chou · Lih-Jung Tseng · Wen-Tar Wu · Pi-Jung Hsu · Kuo-Long Lou

Structural analysis of the functional influence of the surface peptide Gtf-P1 on *Streptococcus mutans* glucosyltransferase C activity

Received: 29 July 2002 / Accepted: 27 January 2003 / Published online: 15 May 2003

Abstract Glucosyltransferases (GtfB/C/D) in *Streptococcus mutans* are responsible for synthesizing water-insoluble and water-soluble glucans from sucrose and play very crucial roles in the formation of dental plaque. A monoclonal antibody against a 19-mer peptide fragment named Gtf-P1 was found in GtfC to reduce the enzyme activity to 50%. However, a similar experiment suggested almost unchanged activity in GtfD, despite of the very high sequence homology between the two enzymes. No further details are yet available to elucidate the biochemical mechanism responsible for such discrimination. For a better understanding of the catalytic behavior of these glucosyltransferases, structural and functional analyses were performed. First, the exact epitope was identified to specify the residue(s) required for monoclonal antibody recognition. The results suggest that the discrimination is determined solely by single residue substitution. Second, based on a combined sequence and secondary structure alignment against known crystal structure of segments from closely related proteins, a three-dimensional homology model for GtfC was built. Structural analysis for the region communicating between Gtf-P1 and the catalytic triad revealed the possibility for an "en bloc" movement of hydrophobic residues, which may transduce the functional influence on enzyme activity from the surface of molecule into the proximity of the active site.

J.-S. Chia
Department of Microbiology, College of Medicine,
National Taiwan University, 10042 Taipei, Taiwan

Y.-S. Shiau · P.-T. Huang · Y.-Y. Shiau · Y.-W. Tsai · H.-C. Chou · L.-J. Tseng · W.-T. Wu · P.-J. Hsu
Graduate Institute of Oral Biology, National Taiwan University,
10042 Taipei, Taiwan

K.-L. Lou (✉)
GIOB, NTUMC,
Chang-Teh Str. 1, 10042 Taipei, Taiwan
e-mail: kllou@ha.mc.ntu.edu.tw
Tel.: +886-2-23562340, Fax: +886-2-23820785

Keywords Glucosyltransferases · *Streptococcus mutans* · Homology modeling · En bloc movement · Monoclonal antibody recognition · Dental caries · Gtf-P1

Introduction

Mutans streptococci have been implicated as the principal causative agents of human dental caries. [1] Such bacteria can secrete glucosyltransferases (GTFs; EC 2.4.1.5) to catalyze the formation of glucose polymers (glucan) from sucrose. These polysaccharides enhance the colonization of cariogenic bacteria and promote the formation of dental plaque on tooth surfaces. [1]

Genetic approaches have identified several GTFs of distinct characteristics in oral streptococci including *S. mutans*, *S. sobrinus*, *S. downei*, and *S. gordonii* (for a review, see [2]). *Streptococcus mutans,* the most prevalent *mutans streptococci* isolated from human oral cavities, [3] produces three GTFs: [4, 5, 6, 7, 8, 9] GtfB (162 kDa), GtfC (149 kDa) and GtfD (155 kDa). The first two enzymes synthesize primarily insoluble glucan, whereas the last one exclusively synthesizes a water-soluble form. Studies of the structural and functional relationship of the GTFs from *S. mutans* and *S. sobrinus* have identified several important domains and specific amino acid residues involved in enzyme activities for glucan binding, sucrose hydrolysis and glucan synthesis. [2] First, a C-terminal glucan-binding domain (GBD) is composed of multiple homologous direct repeat segments, approximately 510 residues. [10] GBD was shown to be essential for glucan synthesis but not for sucrase activity. [11, 12] Second, an N-terminal catalytic domain of about 900 amino acids [2] is capable of binding and hydrolyzing sucrose. [13] This region is highly conserved among GTFs.

The active site, or at least part of the residues contributing to the active site, was proposed to be located on a nine-residue fragment containing a catalytic aspartic

acid, which was observed in the stabilized glucosyl–enzyme complex in GTF-I from *S. sobrinus*. [13] Site-directed mutagenesis confirmed the essential role of this Asp residue for sucrase activity in GTFs from *S. mutans*, [14] *S. downei* [15] and from *L. mesenteroides*. [16] Extension up- and downstream of this nine-residue fragment forms a peptide containing 21 residues, named Gtf-P2 or CAT. [7, 9, 17] Primary sequence alignment revealed that this peptide is highly conserved in the amylases and α-glucosidases. [17] Another peptide able to affect the enzyme activity, Gtf-P1, was identified by Funane and coworkers [18] and by our group [17] at almost the same time. Gtf-P1 consists of 19 amino acids.

Our previous data have shown that a monoclonal antibody against a synthetic peptide with identical sequence to Gtf-P1 in GtfC (GtfC-P1) brings the sucrase activity of GtfC down to about 50%, whereas in GtfD the activity for the same assay was found to be unchanged. [17, 19, 20] There is only one different residue between the sequences of Gtf-P1 in GtfC (435 to 453: ANDVDNSNPVVQAEQLNWL) and in GtfD (Val-438 replaced by Ile-426, i.e., 423 to 441: ANDIDNSNPVVQAEQLNWL). How does this minor substitution cause such a drastic functional discrimination?

Undoubtedly, the N-terminal third of the GTFs plays a central role in sucrose splitting and glucan synthesis. However, the direct crystal structural information indicating the subdomain arrangement and the precise residues required for illustrating the chemical details are still unclear. Therefore, in the present study, we first describe the identification of the epitope required for monoclonal antibody recognition, and then, based on the combined sequence and secondary-structure alignment against the known crystal structures of segments from closely related proteins, a 3-D homology model of the catalytic domain of GtfC was generated and analyzed to provide a possible explanation for the functional discrimination mentioned above.

Materials and methods

Preparation of GTF proteins and Gtf-P1 peptide fragments

His-GtfC and His-D, as well as Gtf-P1 and Gtf-P2 from GtfC, were purified with affinity chromatography as described. [17, 20] E1, E2, and E3 are Gtf-P1 peptide fragments synthesized according to the GtfC sequence, for which each peptide fragment occupies a length of about two-fifths of Gtf-P1.

Enzyme-linked immunosorbent assay (ELISA)

96-well polystyrene enzyme immunoassay plates (GIBCO Laboratories, Grand Island, N.Y.) were used for all reactions. Between steps, the wells were washed three times at room temperature with 0.05% Tween-20 in phosphate-buffered saline (PBS; pH 7.4) by using an automatic washer (Tri-Continent Scientific Inc., Grass Valley, Calif.). The wells were coated with either peptide alone (E1, E2, E3; 1 μg/ml in PBS, pH 7.4) or purified His-GtfC/-D (0.5 μg/ml in sodium carbonate buffer, pH 9.8). This was then incubated overnight at 4 °C and blocked with 150 ml of 0.5% BSA (Sigma Chemical Co., St. Louis, Mo.) for 2 h at 37 °C. Anti-GtfC-P1 (an antibody against Gtf-P1 of GtfC, prepared from mice) was added thereafter and incubated at 37 °C for 2 h. After washing six times with PBS/Tween-20, the bound antibody was detected using alkaline phosphatase-conjugated goat anti-mouse IgG (Sigma) in PBS, followed by a *p*-nitrophenylphosphate substrate (Sigma). The optical densities were measured in a microplate reader (Tri-Continent Scientific Inc.) at 405 nm.

Homology modeling

Search for templates

The BLAST algorithm was employed to search in PDB for protein segments with sequences similar to those of GTFs and whose structures can serve as viable structural templates. The crystal structures of three related amylases or glucosyltransferases (*Bacillus Licheniformis* alpha-amylase, BLI; [21] alpha-amylase precursor, VJS; [22] Glycosyltransferase, BPL [21]) that showed the highest scores in the sequence alignments were chosen for the determination of structurally conserved regions (SCRs). The residues of GTFs used for model building were compared to the BLI sequence according to their paired sequence. In addition, immediately after the primary sequence comparison with BLAST, parts of the carboxyl and amino terminal residues of GTFs were eliminated according to the results.

Paired sequence alignment

The GCG program was used to determine the equivalent residues. The residue regions of BLI represented as continuous lines dominantly observed from GCG were employed as appropriate template regions, and the corresponding fragments in the GTFs were chosen for alignment individually. The amino acid sequences of these GTF fragments were then included in the multiple sequence alignment [23, 24] of the appropriate BLI regions to specify the residue numbers for model building.

Model building and residue side chain simulation

Modeling by homology was performed essentially following the procedures previously described. [23, 25, 26, 27, 28, 29] Briefly, the residue fragments of GTFs were chosen according to the results from GCG-paired se-

quence alignment. They were then superimposed onto the crystal coordinates of the Cα atoms of the corresponding SCRs from the BLI structure. This generated the secondary structure and relative positions of the definite structural elements in the chosen residue fragments of the individual GTF models. Junctions between the secondary structural elements were regularized individually by energy minimization to give reasonable geometries. Further hydrophobic interactions between residue side chains were performed and obtained with molecular dynamics and simulated annealing. All the calculations and structure manipulations were performed with the Discover/Insight II molecular simulation and modeling programs (from Accelrys Inc., San Diego, Calif.; 950 release) on a Silicon Graphics Octane/SSE workstation.

Results

Identification of the epitope required for anti-GtfC-P1

In order to analyze the antigenicity of GTFs and the specificity of anti-GtfC-P1, which was prepared according to the primary sequence of Gtf-P1 of GtfC, [17] ELISA tests with various whole proteins or only with peptide fragments were performed. In Fig. 1a, significant differences between the optical densities due to the binding of anti-GtfC-P1 to GtfC and to GtfD were observed. This specificity of anti-GtfC-P1 was further confirmed by the results shown in Fig. 1b, which suggest a much stronger binding affinity of anti-GtfC-P1 for Gtf-P1 than for Gtf-P2. In addition, since Gtf-P1 is a peptide containing 19 residues that exists in both GtfC and GtfD, further analysis to identify the precise epitope for antibody recognition and to determine which factors affect the binding affinity between GtfC and GtfD, is required. Three peptide fragments from Gtf-P1 of GtfC were synthesized: E1, 440 to 449, NSNPVVQAEQ (from N' to C'); E2, 435 to 444, ANDVDNSNPV; E3, 445 to 453, VQAEQLNWL. In Fig. 1c, the binding of anti-GtfC-P1 to E2 is stronger than to the other two fragments, E1 and E3. This shows that the exact epitope required for anti-GtfC-P1 to recognize GtfC is located on the E2 fragment. Comparison of the Gtf-P1 sequences between GtfC and GtfD revealed that a single residue variation, Val-438 in GtfC, is sufficient to result in the difference in binding for anti-GtfC-P1, as shown in Fig. 1c.

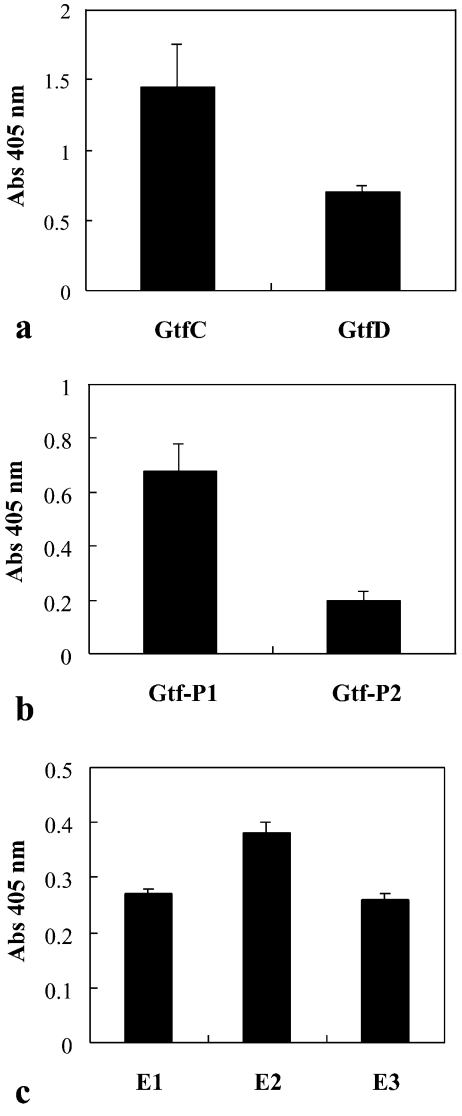

Fig. 1 ELISA results showing the binding ability of anti-GtfC-P1 antibody for BSA–peptide conjugates. **a** GtfC and GtfD, **b** Gtf-P1 and Gtf-P2, **c** intrinsic sequences (E1, E2, E3) of GtfC. 50 μl of BSA–peptide/protein conjugates were coated onto the ELISA plate, whereas 100 μl of anti-GtfC-P1 antibody was then added into the coated wells. The optical densities were detected as the absorbency (Abs) at 405 nm for all the triplicate measurements

Paired sequence and structural alignment

According to the scores of the BLAST template search and the structure–functional properties, *Bacillus Licheniformis* alpha-amylase (BLI) [21] was selected as template protein to build our GtfC homology–structure model. Residue fragments in GtfC used for structural alignment are 428–695 and 886–976 (from the N- to the C-termini). The corresponding residue fragments in BLI applied to create coordinates for GtfC are 191–399 and 33–121, respectively (Fig. 2a, b).

Homology model and side chain interactions

Structural information from our models suggests the subdomain arrangement that coincides with the predictive structural arrangement for GTF-I from *S. downei*. [30] Such a folding pattern of GtfC is also very similar to that of BLI [21] (Fig. 2a, b): a typical Tim-barrel structure composed of eight consecutive units of α/β structural motif (Fig. 2b) by forming the cavity for active sites

(i)

GtfC: 428 GGY **EFLLANDVDNSNPVVQAEQLNWLHFLMNFGNI YANDPDANFD SIRVDAVDNVDADLL 487
BLI : 191 GNY**DYLMY**ADIDYD**HPDVAAE I KRW - - - - - - - GTWYAN**E** - - LQLDGFRLDAVKH I KF SHL 241

GtfC: 488 **Q** IAGD**YLK**AAKG IHKN**DK**AAN**DHLSI** LEAWSYNDTP - - - YL**HDDGDN**MINMDNRLR**LSLL** 544
BLI : 242 **R** - - - **DWVN** - - - - - HVR**EKTGKE**MF**TVAEYWSYDLGALENYLNKTNFNH** SVFD - - - - **VPLH** 289

GtfC: 545 YSLAKPLNQR S G- - MNPL **I** T N**SLVNRTDDNAETAAVPSYSFIRAHDSE**VQDL**I** RN**I I RT** E 602
BLI : 290 YQFHAASTQGGGYDMRKL**LNGTVVSKHP** - - - - - - - **LKSVTFVDNHDTQPGQSLESTVQTW** 342

GtfC: 603 INPNVVGYSFTTEEIKKAFEIYNKDLLATEKKYTHYNT**A**SYALLLTN**KSSVPRVYYGDM** 662
BLI : 343FKP -L AYAFI LTR**ESGYPQVFYGDM** 366

GtfC: 663 FTDDGQYMAHKTINYEAIETLLKARI**KYVSGGQ** 695
BLI : 367 **Y**GTKGDSQR E IPALKHKIEPI LKARK**QY**AYGAQ 399

(ii)

GtfC: 886 AEWG**VTDFEMAPQYVSSTDGSFLDSVIQNGYAFTDRYDLG** I - - - - - **SKPNKYGTADDLVK** 940
BLI: 33 AEHG**ITAVWIPPAYKGTSQADV** - - - - - - - GYGAYDLYDLGEFHQKG**TVRTKYGTKGELQS** 85

GtfC: 941 AIK**ALHSKGIKVMADWVPDQMYALPEKEVVTATRVD** 976
BLI : 86 AIK**SLHSRDINVYGDV V INHKGGADATEDVTAVEVD** 121

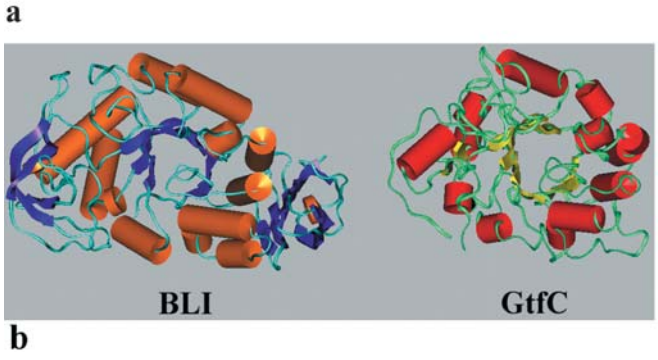

Fig. 2 Comparisons between BLI and GtfC. **a** Sequence homology. *Shadowed* letters denote the identical residues, whereas *bold* ones indicate conservative (positive) substitutions. Homology for two separate fragments (first identical, then positive): (i) GtfC 428–695:23% and 36%; (ii) GtfC 886–976:35% and 44%. **b** Secondary structural elements. Schematic diagrams with secondary structural arrangement are shown to emphasize the Tim-barrel characteristics. The cylinders represent the α-helices, whereas the flat arrows are for the β-strands. The loops connecting in between are drawn with thick lines in distinct colors

(Fig. 3a), as observed in the crystal structures of other closely related sugar-splitting enzymes. [21, 22, 31, 32] The highly conserved 19-residue region, Gtf-P1 (residues 435 to 453 for GtfC), [9, 17] spreads on the surface of the molecule in the structure (Fig. 3a) and forms a fairly long α-helix that protrudes its N-terminal residues into the proximity of Gtf-P2 (residues 468 to 488 for GtfC), including the catalytic Asp-477 (Fig. 3a, b). The structure in Fig. 3a also clearly indicates the exact position and spatial arrangement of the catalytic triad of GtfC (Asp-477, Glu-515, Asp-588).

Molecular dynamics simulation with simulated annealing for the side chain conformations and orientations provided structural information indicating highly ordered hydrophobic interactions between side chains around the region between Gtf-P1 and Gtf-P2 in GtfC (Fig. 3a–d). This suggests a possible mechanism to transduce the influence of antibody binding from the surface of molecule to the active site of enzyme.

Discussion

Our three-dimensional structure model of GtfC in *Streptococcus mutans* revealed the typical Tim-barrel subdomain arrangement for the catalytic domain that is responsible for sugar splitting and substrate binding. Due to the fairly high sequence homology between GtfC and GtfD, it is quite reasonable to predict that the two structures are very similar and that they show the same relative spatial arrangement for their Gtf-P1 and Gtf-P2.

Previous investigations have proposed that the catalytic triad in active sites of GTFs is composed of two aspartates and one glutamate (see previous sections). Our structures provide clear evidence for the spatial orientation of these three residues and how such a catalytic triad organizes to allow the accessibility of the substrate (Figs. 2b and 3a). The catalytic aspartate, for example, Asp-477 in GtfC, is located on Gtf-P2 [13] and therefore at the proper orientation and distance with the other two residues (Glu-515 and Asp-588). Substrates can enter and reach this triad from the wide opening of the cavity formed by the Tim-barrel structure (Figs. 2b and 3a). According to the results from previous studies suggesting that the C-terminal one-third is responsible for the glucan

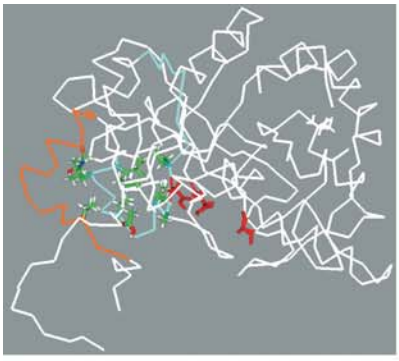

a

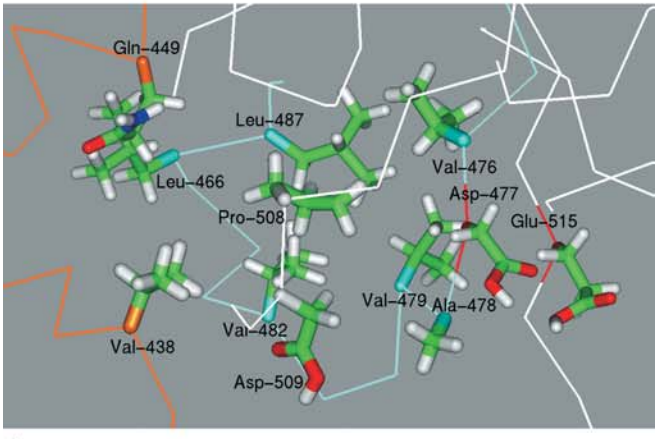

b

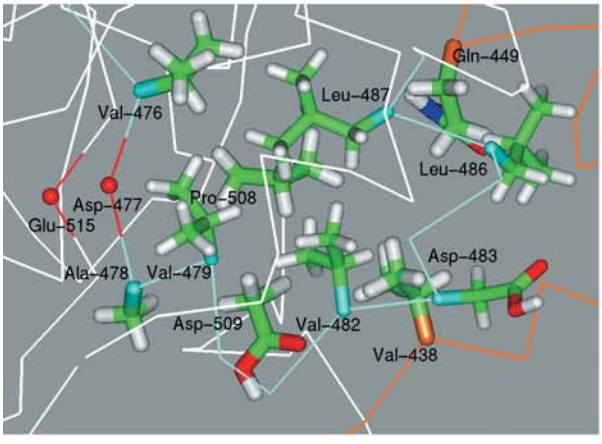

c

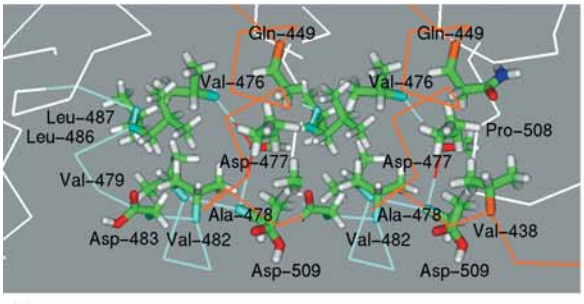

d

binding, [11, 12] we would expect the long molecule of glucan to occupy the remaining part or be outside of this cavity and to be supported by the C-terminal residues. However, due to the elimination of residues for structural alignment, the C-terminal residues of the molecule are not seen in these structures. Therefore, such an assumption remains to be verified.

From our structure, the highly conserved 19-residue fragment, Gtf-P1, [17] is located on the surface of GtfC molecule. Our previous result demonstrated that the monoclonal antibody against this region brings the sucrase activity of GtfB and GtfC down to about 50%. [19] On the other hand, GtfD showed unchanged activity, even slightly increased, for the same assay. [19] It is reasonable to believe that exposure of this 19-residue fragment on the surface of the molecule can lead to a possible "attack" by the antibody. Conformational change of Gtf-P1 induced by such an attack may further affect the catalytic behavior via the protruding residues of this long α-helix into the proximity of Gtf-P2 and the active site (Fig. 3a–d). However, what factors determine the functional discrimination between GtfD and GtfB/C under the same conditions?

To answer this question, we have performed an immunoanalysis using anti-GtfC-P1, a monoclonal antibody against Gtf-P1 of GtfC, to determine what happens during the recognition. First, the specificity of anti-GtfC-P1 between GtfC and GtfD was compared. The results in Fig. 1a confirm that our antibody, which was prepared according to the primary sequence of Gtf-P1 in GtfC, binds more strongly to GtfC than to GtfD. Second, in Fig. 1b, anti-GtfC-P1 binds specifically to Gtf-P1, not Gtf-P2. It seems clear that, due to the different binding affinity, anti-GtfC-P1 recognizes Gtf-P1 in GtfC and then affects the catalytic behavior by disturbing the putative interactions between Gtf-P1 and Gtf-P2. However, we were not fully satisfied with such a simple explanation, especially after we compared the sequence of Gtf-P1 between GtfC and GtfD. We found that only one Gtf-P1 residue is different between GtfC and GtfD: Val-438 for GtfC and Ile-426 for GtfD. Can one similar hydrophobic residue substitution cause such a tremendous discrimination as a consequence of antibody recognition, even if this residue is far away from the active site?

Fig. 3 Side chain interactions between Gtf-P1 and catalytic Asp-477 in GtfC. **a** Cα-tracing of GtfC with the two crucial peptides (Gtf-P1, *orange*; Gtf-P2, *blue*) and the catalytic triad residues (*red*) highlighted to show their relative spatial organization. Side chains for the residues described further in **b** and **c** are also depicted according to their atom types. All the structures in **a**–**d** are viewed with the barrel opening facing down (cf. **b**). **b** Hydrophobic interactions for the area between Val-438 and Asp-477 (*front view*). This structure is viewed with the same orientation as observed in **a**, only enlarged to show the residue side chains in details. **c** Hydrophobic interactions for the area between Val-438 and Asp-477 (*back view*). This structure is viewed by rotation of 180° along a vertical axis as in **b**. **d** Stereo diagram of the residues forming hydrophobic interactions between Val-438 and Asp-477 (*side view*). This structure is viewed by rotation of 90° anticlockwise

There are two ways to examine or to account for this. First, different conformations for Gtf-P1 between GtfC and GtfD might exist, regardless of the fact that only one amino acid residue is changed. Unfortunately, due to the limitations of structure modeling, such details in conformations between GtfC and GtfD could not be compared merely from our 3-D models of GTFs. Thus, we have examined the second possibility. We synthesized three peptide fragments corresponding to parts of Gtf-P1 of GtfC (E1, E2, and E3. For sequences, see Materials and methods and Results). The results shown in Fig. 1c suggest E2 for the strongest affinity, which indicates that the fragment containing Val-438 in GtfC should be able to enhance the antibody recognition, and then further affect the catalysis of GtfC. However, we could not completely exclude the influence of the difference in Gtf-P1 conformation between GtfC and GtfD. This may, hopefully, be further investigated upon the determination of the crystal structures of GTFs in the future.

The next concern is the detailed mechanism by which Val-438 influences GtfC activity from the surface of the molecule upon antibody recognition. This can be illustrated by way of structural analysis for side chain interactions between Gtf-P1 and Gtf-P2. Fig. 3a–d shows the highly ordered hydrophobic interactions between Val-438 and the residues neighboring the catalytic Asp-477, i.e., Val-476, Ala-478 and Val-479. This is an area with uninterrupted hydrophobic interactions between non-polar amino acids, which may form a tightly packed hydrophobic core. The binding of anti-GtfC-P1 to Val-438 may, as speculated from the structural observation illustrated in Fig. 3b–d, induce certain conformational changes of Gtf-P1, which then transduce and draw the flanking valines or alanine residues, together with Asp-477, away from their original positions (putatively similar to en bloc movement). The spatial accuracy of the catalytic triad in GtfC can therefore be altered. This may bring the enzyme activity down to about 50%. Further proof of such a hypothesis also requires the determination of crystal structures of related enzymes.

Our results from the structural and functional analyses have given, at least to a certain extent, although fairly speculative, first direct evidence for the roles of Gtf-P1 in affecting the catalytic function of GTFs. In addition, preliminary data using synthetic Gtf-P1 peptides containing the key residues valine or isoleucine to perform competitive Elisa as reference lead to a similar conclusion. Nevertheless, this work suggests that Gtf-P1 may act as an appropriate candidate for vaccine development in the prevention of human dental caries by abolishing GTF enzyme activity from the surface of the molecules, instead of interacting directly with the active site inside the barrel structure.

Acknowledgements The authors would like to express their most sincere appreciation to Prof. Dr. Robert Huber for his encouragement and discussions in Croatia that enabled part of this project to persist. We are also thankful to Dr. Sofia Strupa and Mr. Willy Stanley for their enthusiasm in suggestions in Rovinj. This work was supported in part by research Grant 89-2314-B-002-555 for LKL from the National Sciences Council of Taiwan and by grants 89c088 and Z403 from NTU. Summer fellowships for visiting scientists from Academia Sinica for years 1999 and 2000 are also gratefully acknowledged.

References

1. Hamada S, Slade HD (1980) Microbiol Rev 44:331–384
2. Monchois V, Willemot RM, Monsan P (1999) FEMS Microbiol Rev 23:131–151
3. Loesche WJ (1986) Microbiol Rev 50:353–380
4. Aoki H, Shiroza T, Hayakawa M, Sato S, Kuramitsu HK (1986) Infect Immunol 53:587–594
5. Hanada N, Kuramitsu HK (1988) Infect Immunol 56:1999–2005
6. Hanada N, Kuramitsu HK (1989) Infect Immunol 57:2079–2085
7. Honda O, Kato C, Kuramitsu HK (1990) J Gen Microbiol 136:2099–2105
8. Shiroza T, Ueda S, Kuramitsu HK (1987) J Bacteriol 169:4263–4270
9. Ueda S, Shiroza T, Kuramitsu HK (1988) Gene 69:101–109
10. Lis M, Shiroza T, Kuramitsu HK (1995) Appl Environ Microbiol 61:2040–2042
11. Abo H, Matsumura T, Kodama T (1991) J Bacteriol 173:989–996
12. Nakano YJ, Kuramitsu HK (1992) J Bacteriol 174:5639–5646
13. Mooser G, Hefta SA, Paxton RJ (1991) J Biol Chem 266:8916–8922
14. Kato C, Nakano Y, Lis M (1992) Biochem Biophys Res Commun 189:1184–1188
15. Devulapalle KS, Goodman SD, Gao Q (1997) Protein Sci 6:2489–2493
16. Monchois V, Remaud-Simeon M, Russel RRB (1997) Appl Microbiol Biotechnol 48:465–472
17. Chia JS, Lin SW, Yang CS, Chen JY (1997) Infect Immunol 65:1126–1130
18. Funane K, Shiraiwa M, Hashimoto K, Ichishima E, Kobayashi M (1993) Biochemistry 32:13696–13702
19. Chia JS, Lin RH, Lin SW, Chen JY (1993) Infect Immunol 61:4689–4695
20. Chia JS, Yang CS, Chen JY (1998) Infect Immunol 66:4797–4803
21. Machius M, Wiegand G, Huber R (1995) J Mol Biol 246:545–559
22. Hwang KY, Song HK, Chang C (1997) Mol Cells 7:251–258
23. Siezen RJ, de Vos WM, Leunissen JA (1991) Protein Eng 4:719–737
24. Siezen RJ, Rollema HS, Kuipers OP (1995) Protein Eng 8:117–125
25. Tsai YW, Chia JS, Shiau YY, Chou HC, Liaw YC, Lou KL (2000) FEMS Microbiol Lett 188:75–79
26. Lou KL, Chou HC, Tsai YW, Shiau YS, Huang PT, Chen TY, Shiau YY, French RJ (2001) J Mol Model 7:20–25
27. Huang PT, Chen TY, Liou HH, Lin TB, Spatz HC, Tseng LJ, Shiau YY, Lou KL (2002) Recept Channels 8:79–85
28. Lou KL, Huang PT, Shiau YS, Shiau YY (2002) J Mol Recognit 15:175–179
29. Shiau YS, Lin TB, Liou HH, Huang PT, Lou KL, Shiau YY (2002) J Mol Model 8:243–247
30. Monchois V, Lakey JH, Russell RR (1999) FEMS Microbiol Lett 177:243–248
31. Jespersen HM, MacGregor AE, Henrissat B (1996) J Protein Chem 12:791–805
32. MacGregor EA, Jespersen HM, Svensson B (1996) FEBS Lett 378:263–266